Nonpeptide Somatostatin Receptor Agonists Specifically Target Ocular Neovascularization via the Somatostatin Type 2 Receptor

Stela S. Palii,[1] Aqeela Afzal,[1] Lynn C. Shaw,[1] Hao Pan,[1] Sergio Caballero,[1] Rehae C. Miller,[2] Simona Jurczyk,[3] Jean-Claude Reubi,[4] Yufei Tan,[5] Guenther Hochhaus,[5] Henry Edelhauser,[6] Dayle Geroski,[6] Gideon Shapiro,[3] and Maria B. Grant[1]

Purpose. To define the molecular pharmacology underlying the antiangiogenic effects of nonpeptide imidazolidine-2,4-dione somatostatin receptor agonists (NISAs) and evaluate the efficacy of NISA in ocular versus systemic delivery routes in ocular disease models.

Methods. Functional inhibitory effects of the NISAs and the somatostatin peptide analogue octreotide were evaluated in vitro by chemotaxis, proliferation, and tube-formation assays. The oxygen-induced retinopathy (OIR) model and the laser model of choroidal neovascularization (CNV) were used to test the in vivo efficacy of NISAs. Transscleral permeability of a candidate NISA was also measured.

Results. NISAs inhibited growth factor–induced HREC proliferation, migration and tube formation with submicromolar potencies (IC_{50}, 0.1–1.0 μM) comparable to octreotide. In the OIR model, systemic administration of the NISAs RFE-007 and RFE-011 inhibited retinal neovascularization in a dose-dependent manner, comparable to octreotide. In the CNV model, intravitreal RFE-011 resulted in a 56% reduction ($P < 0.01$) in CNV lesion area, whereas systemic administration resulted in a 35% reduction ($P < 0.05$) in lesion area. RFE-011 demonstrated transscleral penetration.

Conclusions. Micromolar concentrations of octreotide and NISAs are necessary for antiangiogenic effects, whereas nanomolar concentrations are effective for endocrine inhibition. This suggests that the antiangiogenic activity of NISAs and octreotide is mediated by an overall much less efficient downstream coupling mechanism than is growth hormone release. As a result, the intravitreal or transscleral route of administration should be seriously considered for future clinical studies of SSTR2 agonists used for treatment of ocular neovascularization to ensure efficacious concentrations in the target retinal and choroidal tissue. (*Invest Ophthalmol Vis Sci.* 2008;49:5094–5102) DOI:10.1167/iovs.08-2289

Neovascular ocular diseases represent a major health threat to all age groups and especially the rapidly increasing diabetic and aging patient populations. Proliferative diabetic retinopathy (PDR) is the leading cause of blindness that afflicts the young-to-middle age population in the Western world, and 21 million people have diabetes in the United States alone.[1] Exudative, or wet, age-related macular degeneration (AMD) is the leading cause of blindness and the most prevalent neovascular disease in the elderly, affecting more than 500,000 people in the United States.[2] Other neovascular ocular diseases such as retinopathy of prematurity (ROP), the major cause of blindness in children younger than 7 years, and retinal vascular occlusions (RVOs) are less prevalent but extremely debilitating conditions. Although the vascular bed and distribution of tissue disease varies across these ocular diseases, the proliferation of aberrant blood vessels is common to all.

Prior therapies for neovascular ocular disease have relied exclusively on laser photocoagulation, either directly (e.g., panretinal photocoagulation [PRP] for PDR) or in tandem with the photosensitizing porphyrin verteporfin (Visudyne; Novartis Pharmaceuticals, Inc., East Hanover, NJ) as a photodynamic therapy (for exudative AMD). Although PRP remains the standard of care for PDR, VEGF inhibitor drugs, particularly the humanized anti-VEGF antibody fragment ranibizumab (Lucentis; Genentech, South San Francisco, CA), have recently been established as effective therapeutics for exudative AMD. Even with this advancement, there remains a critical need to add new pharmacologic treatment modalities such as monotherapies and synergistic combination therapies with anti-VEGF drugs for continued improvement in the management of neovascular diseases.

Somatostatin was originally identified in the hypothalamus as the endogenous inhibitory factor of pituitary growth hormone (GH) secretion.[3] Somatostatin drugs have long been recognized as having promise for treating PDR by a systemic mechanism of action involving pituitary somatostatin receptor (SSTR) activation and inhibition of the GH-insulin-like growth factor (IGF)-1 axis. Unfortunately, the stable somatostatin peptide analogue octreotide, which is clinically effective in treating the disorder of GH and IGF-1 hypersecretion (acromegaly), has shown equivocal results in clinical trials for DR. We considered possible reasons for the variation in clinical outcomes. First, SSTRs have been identified on angiogenic tumor blood vessels, and the antiangiogenic activity of somatostatin agonists has been described in vitro, indicating a paracrine mechanism of action. Thus, octreotide's therapeutic effects are hypothesized to be mediated by SSTR activation directly on the ocular target tissue. Furthermore, this paracrine effect potentially involves SSTR subtypes other than SSTR2 and -5, which mediate GH inhibition and for which octreotide is selective. Second, the peptide octreotide does not cross the blood–brain barrier

From the Departments of [1]Pharmacology and Therapeutics, [2]Ophthalmology, and [5]Pharmaceutics, University of Florida, Gainesville, Florida; [3]RFE Pharma, Alachua, Florida; the [4]Division of Cell Biology and Experimental Cancer Research, Institute of Pathology, University of Bern, Bern, Switzerland; and the [6]Department of Ophthalmology, Emory University, Atlanta, Georgia.

Supported by National Eye Institute Grant EY015952 (MBG, GS).

Submitted for publication May 13, 2008; revised June 27, 2008; accepted August 28, 2008.

Disclosure: **S.S. Palii**, None; **A. Afzal**, None; **L.C. Shaw**, None; **H. Pan**, None; **S. Caballero**, None; **R.C. Miller**, None; **S. Jurczyk**, RFE Pharma (E); **J.-C. Reubi**, None; **Y. Tan**, None; **G. Hochhaus**, None; **H. Edelhauser**, None; **D. Geroski**, None; **G. Shapiro**, RFE Pharma (E, P); **M.B. Grant**, None

The publication costs of this article were defrayed in part by page charge payment. This article must therefore be marked "*advertisement*" in accordance with 18 U.S.C. §1734 solely to indicate this fact.

Corresponding author: Maria B. Grant, Pharmacology and Therapeutics, University of Florida, PO Box 100267, Gainesville, FL 32610-0267; grantma@pharmacology.ufl.edu.

and would have access only where there is disruption of the blood–retinal barrier, thus limiting the amount of drug reaching the retinal target tissue. Moreover, this could result in a higher dose requirement for octreotide to be efficacious in DR versus acromegaly.

Recently, a novel class of highly active nonpeptide imidazolidine-2,4-dione SSTR agonists (NISAs; Fig. 1) has been described. The lipophilicity of these NISA compounds can vary, and a range of analogues display nanomolar potency at SSTR2 receptors with varying selectivity at SSTR3. In the present study, we used this NISA class of compounds, together with selective SSTR2 and -3 antagonists, to investigate the effects of subtype selectivity and lipophilicity on the somatostatinergic ocular antiangiogenic function using in vitro and in vivo ocular model systems. In addition, the therapeutic potential of the selected NISA compounds, in particular RFE-011, was evaluated in vivo in neovascular ocular disease and ocular toxicity models.

Methods

Drugs

Experimental NISAs were synthesized and provided by RFE Pharma (Alachua, FL). The general structure of NISA is shown in Figure 1. For in vivo administration in mice, test solutions of salt forms of the test compounds were prepared in water. Hydrochloride salt forms of the NISA compounds and octreotide acetate were injected intraperitoneally in volumes of 50 μL or less per mouse at doses of 1.0 or 3.0 mg/kg body weight twice daily, starting from postnatal day 12 for the pups in the oxygen-induced retinopathy (OIR) model. Hydrochloride and palmitate salt solutions of RFE-011 were supplied by RFE Pharma in ready-to-use isotonic formulations and were injected intravitreally in 30-μL volumes for the rabbit toxicity studies. Drug quality control was ensured by the specificity of the synthetic pathway and verified by HPLC, NMR, and MS analysis. All solutions for intravitreal injections were stored in conformity with the manufacturer's instructions at 20 to 23°C. Control mice were injected with vehicle alone.

In Vitro Receptor Binding Studies

To assess SSTR-binding affinities and subtype specificities, cells stably expressing human SSTR1, -2, -3, -4, and -5 (SSTR1 and -5, CHO-K1 cells; SSTR2 to -4, CCL39 cells) were grown as described previously.[4] Cell membrane pellets were prepared and receptor autoradiography was performed on pellet sections (mounted on microscope slides), as described previously.[4] Complete displacement experiments were performed with the universal SST radioligand ^{125}I-[Leu^8, d-Trp^{22}, Tyr^{25}]-somatostatin-28, with increasing concentrations of RFE-007 ranging from 0.1 to 1000 nM. Somatostatin-28 was run in parallel as the control, with the same increasing concentrations. IC_{50} was calculated by using a computer-assisted image-processing system. Tissue standards (autoradiographic ^{125}I microscales; GE Healthcare, Piscataway, NJ), containing known amounts of isotopes and cross-calibrated to tissue equivalent ligand concentrations, were used for quantification.

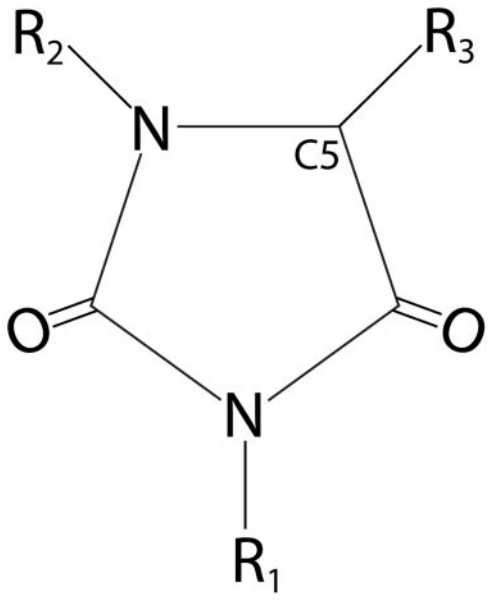

Figure 1. Structure of NISA. Highly selective SSTR2/SSTR3 NISAs exert dramatic inhibitory effects in both in vitro and in vivo angiogenesis models.

Cell Culture

Human donor eyes were obtained from the National Disease Resource Interchange (Philadelphia, PA) within 36 hours of death. Primary cell cultures were established as published previously.[5]

RNA Extraction and Real-Time PCR

Pooled HRECs from a minimum of four different donors were seeded to 75% confluence in six-well dishes and allowed to attach and resume active growth over a period of 5 to 7 days. During this time, they were fed with fresh complete medium every 24 hours. Total RNA was isolated from the HRECs (RNeasy kit; Qiagen, Valencia, CA) and treated with DNase I before final elution to eliminate any DNA contamination, according to the manufacturer's instructions. Complementary DNA synthesis was performed with a first-strand DNA synthesis kit (QuantiScript; Qiagen) that included a treatment for the elimination of genomic DNA. Real-time PCR primer mixes for SSTR1 to -5 (QuantiTect primer assays; Qiagen) were used according to the manufacturer's instructions. The β-actin primer mix was purchased from Ambion (Austin, TX). The analysis was performed by quantitative real-time PCR and SYBR Green (DNA Engine Opticon 2 system; MJ Research, Reno, NV). RNA reaction mixtures were incubated at 48°C for 30 minutes followed by 95°C for 15 minutes and amplification in 40 cycles at 95°C for 15 seconds and then 60°C for 60 seconds. The data were normalized relative to β-actin mRNA levels.

HREC Proliferation Assays

The HRECs were seeded at 3×10^5 cells per well in 96-well plates. All experiments were performed in triplicate. Before each treatment the cells were serum starved for 24 to 48 hours in a medium consisting of 50% Ham's F-12, 50% low-glucose DMEM with antibiotics and antimycotics and 0.5% FBS. The cells were then switched to either complete HREC medium with 10% FBS (positive control) or fresh 0.5% FBS medium, with or without test compounds. Control cultures received medium with the inhibitor vehicle (PBS). Bromodeoxyuridine (BrdU) was added at this time. Cell proliferation was determined after 48 hours of treatment by measuring BrdU incorporation with a kit (Calbiochem, San Diego, CA) according to the manufacturer's instructions.

HREC Migration Studies

Chemotaxis was performed in modified (blind-well) Boyden chambers (NeuroProbe, Gaithersburg, MD), as previously described.[6] The SSTR agonists were tested at concentrations ranging from 1×10^{-5} to 1×10^{-10} M in log steps. These were prepared in the presence of a growth factor (GF) cocktail consisting of 10 ng/mL Long R3-IGF-1 (Cell Sciences, Canton, MA), 50 ng/mL VEGF (R&D Systems, Minneapolis, MN), and 25 ng/mL FGF-2 (Sigma-Aldrich, St. Louis, MO), which in combination served as the positive control. All conditions were tested in triplicate.

HREC Tube-Formation Studies

HRECs were pooled from three donors and seeded at 1.5×10^4 cells/well of a 96-well GF–poor, coated assay plate (Matrigel; BD Biosciences, San Jose, CA). The cells were plated in a GF cocktail

medium containing DMEM (MediaTech, Herndon, VA), 25 ng/mL FGF-2, 25 ng/mL VEGF, and 10 ng/mL human Long R3-IGF-1.[7] The cells were pretreated for 30 minutes with concentrations of RFE-011 or octreotide (GenScript Corp., Piscataway, NJ) ranging from 1×10^{-5} to 1×10^{-8} M. The cells were then exposed to either the SSTR-2 antagonist cyclosomatostatin (cSOM; Bachem, Torrance, CA) or the highly selective SSTR3 antagonist BN81658 at 1×10^{-6} M.[8,9] Tube formation was monitored over 24 hours by digital image capture with a microscope (Carl Zeiss Meditec, Dublin, CA).

Experimental Animals

All animal procedures used were in compliance with the NIH Guide for the Care and Use of Laboratory Animals and the ARVO Statement for the Use of Animals in Ophthalmic and Vision Research and were approved by the University of Florida Institutional Animal Care and Use Committee. Mice were purchased from Jackson Laboratory (Bar Harbor, ME).

Mouse Oxygen-Induced Retinopathy Model

Neovascularization in neonatal mice was induced in heterozygous C57BL/6J mice (Jackson Laboratory) by using the OIR model, as previously described.[10,11]

Induction of Choroidal Neovascularization by Laser Injury

CNV was induced in mice by laser rupture of Bruch's membrane, as previously described.[12]

Rabbit Eye Toxicity Studies

Healthy New Zealand White rabbits (1.5 kg females, $n = 9$) were purchased from Harlan (Indianapolis, IN). The rabbits were injected intravitreally with 30 μL of drug. Two different concentrations were tested for each of the drug formulations. Isotonic RFE-011 (3 mg/mL and 10 mg/mL) hydrochloride and palmitate salt formulations (7 mg/mL and 21 mg/mL, respectively) were prepared in 200 mM mannitol. The control eyes received an equal volume (30 μL) of the 200-mM mannitol solution (vehicle). Table 1 shows the allocation of animals for each treatment group.

The rabbits were euthanatized at either 24 hours or 1 week, and the eyes were enucleated, placed in Bouin's fixative for 4 hours to harden, processed, and stained with hematoxylin-eosin. For each eye, five sections (5 μm thick) taken at five levels 100 μm apart were examined by light microscopy at low (35×) and high (100×) magnifications. Each eye was divided into four equal quadrants and a first evaluation was performed to document the presence (+) or the absence (−) of ocular disease.

A relative scale from 0 to 5 was adopted, with a score of 0 assigned to normal retinas and a score of 5 assigned to the gravest pathologic manifestations. The scoring of the slides was performed by two individuals masked to the treatment conditions. To ensure an accurate evaluation of the drugs' effects, the retinal area was visually estimated in percentages of total retinal surface. After all the data were recorded, the slides were examined by a third individual aware of the treatment conditions. Sections from the same eye were compared to each other to assess whether the same morphologic changes (or the absence thereof) could be seen throughout the entire set of five sections per eye. The average percentage of each score for the entire eye (five sections, taken at five levels 100 μm apart) was calculated to express the occurrence of each disease score for each rabbit in the group. Then, the mean values were calculated for each score (0–5) for all the experimental groups. The data were plotted and evaluated statistically by the Student's *t*-test (Prism 3.0; GraphPad Software, San Diego, CA). A difference with a probability of 5% ($P \leq 0.05$) was considered statistically significant.

In Vitro Transscleral Flux Studies

In vitro flux studies were conducted to estimate the transscleral permeability of RFE-011. For these experiments, sclerae were obtained from the eyes of New Zealand White rabbits weighing 1.0 to 1.5 kg. The rabbits were anesthetized and then killed by an intracardiac injection of pentobarbital sodium (97.2 mg/kg). The eyes were enucleated and adherent extraocular tissues, including conjunctiva and periorbital muscles, were carefully removed. The episclera and uvea were removed with a cotton swab to isolate the bare sclera. Scleral disks of 15 to 20 mm in diameter were excised from the superior temporal section of the globe, 12 to 15 mm posterior to the limbus.

The excised sclera was mounted horizontally, choroid side down, in a specially designed Lucite perfusion chamber, as previously described.[13–15] Briefly, the sclera was clamped between two 2.5-mm wide (~1-mm thick) cylindrical Sylgard rings (Dow Corning, Inc., Midland, MI) cut to the size of the chamber opening to prevent lateral leakage and scleral edge damage. The sclera divides the perfusion chamber into upper and lower compartments. The donor compartment (upper chamber), which serves as a depot, has a volume of 600 μL. The volume of the lower (receiver) chamber is 500 μL. Physiologic saline (BSS; Alcon Laboratories, Inc., Fort Worth, TX) was perfused through the lower chamber at a rate of 0.03 mL/min. Fluid mixing was achieved in the lower chamber with a magnetic microstir bar while the chamber was placed on a magnetic stir plate. The tissue was perfused for 15 to 30 minutes to verify that no leaks were present before the test agent (H_2O, carboxyfluorescein, dexamethasone-fluorescein, or RFE-011) was added to the upper chamber.

The RFE-011 hydrochloride salt, 140 μL of a 10^{-4} M solution in aqueous 200 mM mannitol solution (pH 5.5), was added to the episcleral surface 15 to 30 minutes after the sclera was mounted in the chamber. The temperature of the water-jacketed perfusion chamber was maintained at 37°C by a circulating water bath.

Perfusate samples were collected by a fraction collector (Isco, Lincoln, NE) at 15-minute intervals. The content of the perfusate

TABLE 1. Dose Groups for the Intravitreal Rabbit Eye Toxicity Study of RFE-011 Drug Formulations

Group 1, 24-Hour Time Point ($n = 9$)					
Subgroup 1-1 ($n = 3$)		**Subgroup 1-2 ($n = 3$)**		**Subgroup 1-3 ($n = 3$)**	
Left Eye	**Right Eye**	**Left Eye**	**Right Eye**	**Left Eye**	**Right Eye**
Vehicle	Palmitate, 21 mg/mL	Vehicle	HCl, 10 mg/mL	Palmitate, 7 mg/mL	HCl, 3 mg/mL
Group 2, 1-Week Time Point ($n = 9$)					
Subgroup 2-1 ($n = 3$)		**Subgroup 2-2 ($n = 3$)**		**Subgroup 2-3 ($n = 3$)**	
Left Eye	**Right Eye**	**Left Eye**	**Right Eye**	**Left Eye**	**Right Eye**
Vehicle	Palmitate, 21 mg/mL	Vehicle	HCl, 10 mg/mL	Palmitate, 7 mg/mL	HCl, 3 mg/mL

samples was determined by HPLC-MS analysis calibrated over the range of concentrations tested. The steady state permeability constant (K_{trans}) was calculated as:

$$K_{trans} = \frac{R_{total}}{(t)(A)} \times \frac{1}{[D]} \quad (1)$$

where R_{total} is the total amount of solute in the receiver effluent per collected fraction, t is the fraction collection time (in seconds), A is the area of exposed sclera (0.385 cm^2), and $[D]$ is the concentration of drug in the donor chamber. The permeability constant represents the steady state flux normalized by donor concentration.

Data Collection and Statistical Analysis

Inhibitor treatment data sets for cultured HRECs were individually compared to their respective controls by the paired Student's *t*-test (Prism 3.0). $P \leq 0.05$ was considered to be significant. In the experiments in which one treatment was compared with several others, nonparametric, one-way ANOVA was used (GraphPad Software). In the animal studies, all data among the various groups were compared by ANOVA. For morphometric area and volume measurements ImageJ software (available by ftp at zippy.nimh.nih.gov/ or at http://rsb.info.nih.gov/nih-image; developed by Wayne Rasband, National Institutes of Health, Bethesda, MD) was used on calibrated digital image captures. For the retinal toxicity studies, the mean values were calculated for each pathology score (0–5) for all the experimental groups. The data were plotted and evaluated statistically with Student's *t*-test (Prism 3.0; GraphPad Software). A difference $P \leq 0.05$ was considered statistically significant.

Results

SSTR Expression in HRECs

HRECs expressed SSTR1 to -3 (Fig. 2), with SSTR1 being the predominant isoform, followed by SSTR2 and a relatively low level of SSTR3. No SSTR4 or -5 expression was detected under the examined experimental conditions and whether the cells were in a state of proliferation or quiescence did not alter the receptor subtype expressed (data not shown). Thus, HRECs represented an appropriate endothelial cell population to examine the effects of peptidomimetic NISA analogues with high SSTR2 specificity and moderate SSTR3 affinity.

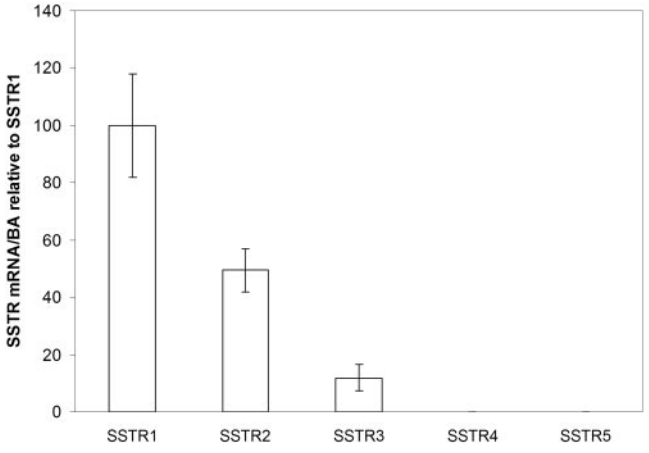

Figure 2. SSTRs expression in HRECs. Actively growing HRECs pooled from at least four donor eyes were used for these experiments, and the expression of the respective receptors was measured from equal starting volumes of cDNA reactions in triplicate. Data were normalized against β-actin mRNA content and relative to SSTR1 (set at 100%). Representative data from four independent experiments are shown.

Table 2. Normalized SSTR Binding Data

Compound	SSTR1	SSTR2	SSTR3	SSTR4	SSTR5
SST-14	5.2	2.7	7.7	5.6	4.0
Octreotide	>10,000	2.0	187	>1,000	22
RFE-007	>10,000	0.8	450	>1,000	470
RFE-008	>1,000	2.3	>100	>1,000	>10
RFE-011	>10,000	3.0	180	>1,000	>100

Affinity profiles (nM IC_{50} values) across human SSTRs for native SST-14, octreotide, and NISA compounds RFE-007, RFE-008, and RFE-011.

SSTR Binding Data for NISAs

Binding affinities for were obtained by IC_{50} measurements in triplicate by using somatostatin-14 (SST-14) as an internal standard (attributed value of 1). For the NISA compounds examined, the affinities for SSTR2 were the highest, with moderate affinity IC_{50} (<10) obtained for SSTR3 and very low (<1000) IC_{50} for SSTR1 and -4. Therefore, the nonpeptide small molecules displayed SSTR2 affinities comparable to that of the natural peptide agonist SST-14 (Table 2).

Effect of NISAs on HREC Proliferation

The efficacy of SSTR agonists in inhibiting endothelial cell proliferation was examined in vitro in cultured HRECs. Figure 3 shows the results of the comparison of the antiproliferative efficacy of three of the RFE Pharma compounds (RFE-007, RFE-008, and RFE-011) to octreotide. The data are normalized to BrdU incorporation in cells exposed to a GF cocktail alone and represent the combined results of three separate experiments. All NISA compounds showed antiproliferative effects comparable to octreotide.

NISA Inhibition of HREC Chemotaxis

We investigated whether NISAs may also have direct effects on endothelial cell chemotaxis in response to GF stimulation. As

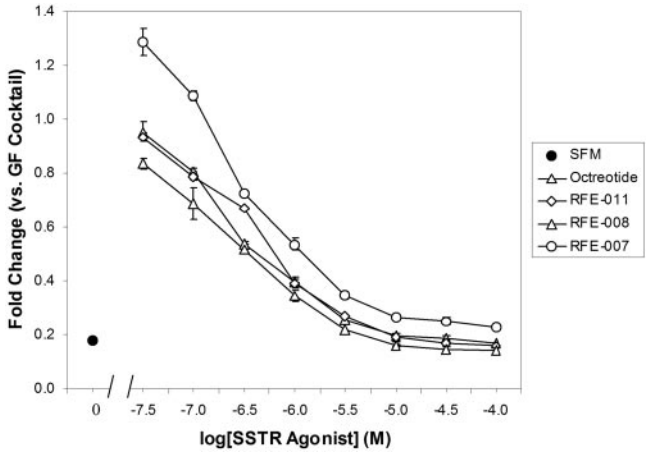

Figure 3. The effects of RFE-007, -008, and -011 on endothelial cell proliferation in response to GF stimulation. HRECs were exposed to a GF cocktail consisting of 10 ng/mL IGF-1, 100 ng/mL VEGF, and 25 ng/mL FGF-2. To this GF cocktail were added serial dilutions of the SSTR agonists. Cells treated with serum-free medium (SFM) alone served as the negative control, and cells exposed to a GF cocktail alone served as the positive control. All conditions were tested in triplicate, and repeated using early-passage cells from a minimum of three donors.

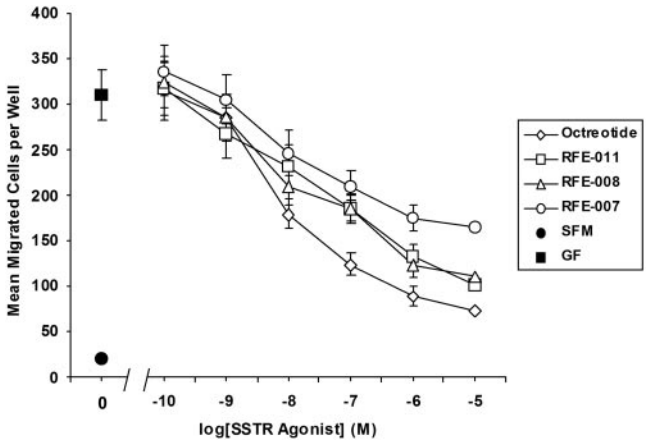

FIGURE 4. The effects of RFE-007, -008, and -011 on endothelial cell chemotaxis in response to GF stimulation. All three compounds showed a concentration-dependent inhibitory effect on migration and were effective at inhibiting GF-induced endothelial cell chemotaxis. All conditions were tested in triplicate and repeated using early-passage cells from a minimum of three donors.

shown in Figure 4, RFE-008 and RFE-011 were equally effective in inhibiting GF-induced endothelial cell chemotaxis, but were slightly less so than octreotide. RFE-007 was the least effective of the compounds tested, yet still showed a concentration-dependent inhibitory effect on migration.

NISAs and Octreotide Inhibition of Tube Formation

RFE-011 showed direct inhibitory effects on endothelial cell tube formation on synthetic basement membrane (Matrigel; BD Biosciences; Fig. 5A); similarly, octreotide inhibited tube formation (Fig. 5E). However, when HRECs were pretreated with RFE-011 (10^{-7} M) the presence of the SSTR2 antagonist cSOM (Fig. 5B) tube formation was restored. This effect was also observed when octreotide was combined with cSOM (Fig. 5F). RFE-011 showed direct inhibitory effects on endothelial cell tube formation on the synthetic matrix. Although RFE-011 showed a trend toward reversal of this effect with cSOM and the SSTR3 antagonist BN81658, the data were equivocal. The pan-SSTR agonist SST-14, which has nanomolar activity across all SSTR subtypes, inhibited tube formation at concentrations comparable to octreotide and RFE-011 (data not shown). Also, the inhibitory effect of octreotide on proliferation in the more robust human microvascular endothelial cells of the lung was effectively blocked by pretreatment with cSOM (10^{-6} M) but not with BN81658 (10^{-6} M; data not shown). These results indicate that the SSTR2 receptor is the predominant inhibitor of tube formation and antiproliferative effects.

Human Transscleral Permeability Studies

The results of the flux studies are shown in Table 3. After a brief lag period, RFE-011 flux across the rabbit sclera peaked at 3 to 5 hours and then gradually diminished over the remainder of the experiment. Calculating K_{trans} over the 2- to 4-hour perfusion period results in an estimated K_{trans} of 3.8×10^{-6} cm/s for RFE-011.

NISAs Reduce Preretinal Neovascularization in the OIR Model

We used the OIR model to assess the in vivo efficacy of the NISAs showing the greatest in vitro efficacy and compared their action to that of systemic octreotide administration. All compounds were tested at doses of 1 or 3 mg/kg/d and were administered twice daily by intraperitoneal injection. Selected pups were injected with vehicle alone (sterile saline) as control. Figure 6 illustrates the quantitative evaluation of preretinal nuclei and demonstrates that all compounds tested resulted in a concentration-dependent decrease in the number of preretinal endothelial cells. RFE-008 was as effective as octreotide in reducing preretinal neovascularization in this in vivo model. Although RFE-011 was less effective, it still resulted in reduction of preretinal neovascularization.

Effect of NISAs on Experimental CNV

As shown in Figure 7, a RFE-011-palmitate formulation was given by intravitreal injection and reduced CNV lesion size in a dose-dependent manner compared to control conditions and with an efficacy similar to octreotide.

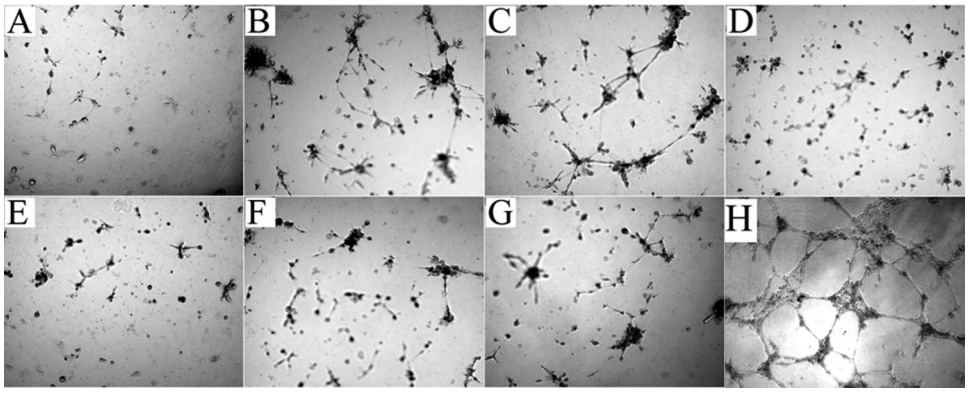

FIGURE 5. HREC tube formation was inhibited by RFE-011 (10^{-7} M) (**A**) and octreotide (10^{-7} M) (**E**); however, in the presence of RFE-011 and the SSTR2 antagonist cSOM (**B**), modest restoration of tube formation was observed. This response was also observed with octreotide and the SSTR2 antagonist cSOM (**F**). Similarly when the HRECs were exposed to RFE-011 and the SSTR3 antagonist BN81658 (**C**), tube formation was partially restored. This effect was also observed with octreotide and BN81658 (**G**). These results support the importance of SSTR2 activity in inhibiting in vitro angiogenesis with equivocal results versus SSTR3. The negative control (**D**) was grown in SFM, whereas the positive control (**H**) was in GF medium.

TABLE 3. Transscleral Permeability Expressed as K_{trans}

Solute	Molecular Weight	K_{trans} (10^{-6} cm/s)
H_2O	18	51.8 ± 18
Carboxyfluorescein	317	9.93 ± 3.5
RFE-011	666	3.8
Dexamethasone-fl	841	1.64 ± 0.17

Results of the transscleral permeability measurements for various solutes show that the NISA RFE-011 can readily cross the sclera to effect its action via topical delivery.

Intravitreal Rabbit Eye Toxicity of RFE-011 Formulations

Because our studies suggest that a more efficacious therapeutic approach would be local delivery rather than systemic administration, we evaluated the safety considerations of such an approach. Thus, two salt forms, an immediate release hydrochloride form and a slow release palmitate form of RFE-011, were investigated for possible ocular toxicity. The intravitreal toxicity of both formulations of RFE-011 is shown in Figure 8. The abnormalities observed were relatively mild and consisted of subtle morphologic changes with minimal disruption of the retinal layers (nerve fiber layer and photoreceptor inner and outer segments). In both the control and the experimental group, retinal cells appeared healthy, with no evidence of cellular necrosis. For both RFE-011 formulations, no significant abnormalities were observed at the concentrations of 3 or 7 mg/mL or at either of the time points tested (24 hours or 1 week).

DISCUSSION

The results of this study demonstrate that among SSTR1, -2, and -3, all expressed by HRECs, SSTR2 is the predominant mediator of functional ocular antiangiogenic effects. The concentrations of SSTR2 agonists for antiangiogenic activity are, however, two to three orders of magnitude higher than those of their current clinical use as GH-release inhibitors. This finding indicates that ocular administration of SSTR2 agonists should be considered for future clinical studies to achieve higher efficacious concentrations. In this regard, the novel class of potent SSTR2-selective NISAs we have tested demonstrated efficacy comparable to octreotide, in vitro and in vivo. These NISAs were not only highly efficacious but also were nontoxic when administered by intravitreal injections and were amenable to transscleral delivery.

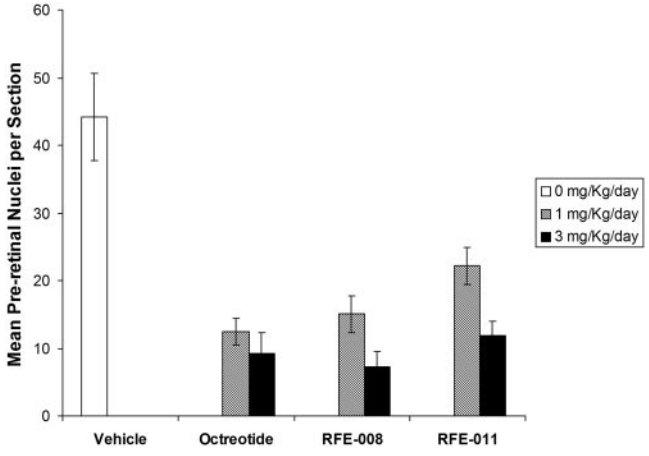

FIGURE 6. Graphic representation of the quantitative results from tests of SSTR agonists in the neonatal mouse model of OIR. All the compounds tested significantly reduced the degree of preretinal neovascularization compared with the vehicle control. Representative results of three independent experiments are shown.

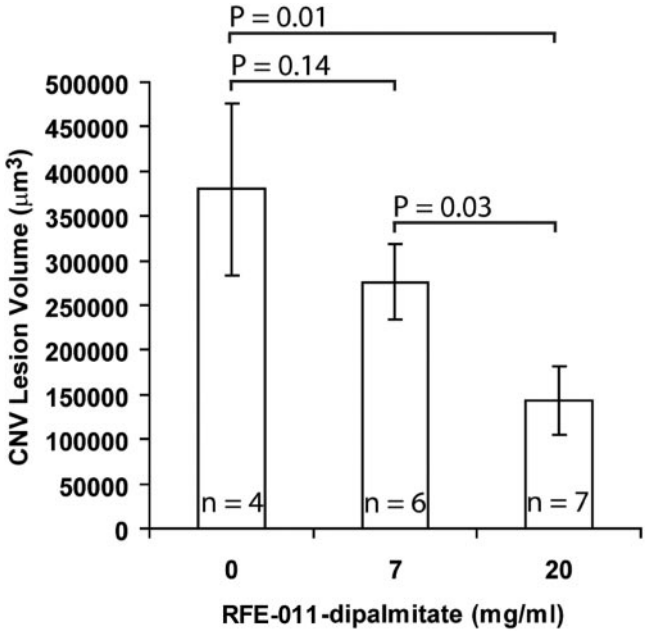

FIGURE 7. The effect of intravitreal SSTR analogue on CNV lesion area after laser rupture of Bruch's membrane. RFE -011 given as two separate injections reduced CNV lesion size compared to vehicle injected eyes. Representative results of three independent experiments are shown.

The original mechanistic hypothesis for somatostatin drug therapy for PDR was based on the potent inhibition of the GH–IGF1 axis. Indeed, systemic therapy with octreotide has been described to result in regression of neovascularization and also improve visual acuity in patients with advanced DR.[16,17] However, the clinical results have not been uniformly positive, and the most favorable results have been observed in patients receiving high dosage regimens, well above doses that effectively lower systemic GH in patients with acromegaly. These observations suggest that the clinical therapeutic effect of octreotide in DR may be due, not to the endocrine mechanism, but rather to a direct effect on SSTRs in ocular target tissues.

Before our studies, the need for high systemic doses of octreotide for clinical efficacy in DR and ultimately other neovascular ocular diseases was explainable by one or more of the following: Octreotide's effect is mediated by a SSTR subtype other than SSTR2; octreotide inadequately penetrates the blood–retinal barrier after systemic administration; or the SSTR2-mediated anti-angiogenic effect is less efficient than GH inhibition. The findings of our in vitro and in vivo model studies with the novel class of potent nonpeptide SSTR agonists point to the third explanation and the need for a new treatment regimen for drug-based therapy for neovascular ocular disease with SSTR agonists.

Diverse in vitro and in vivo mechanistic and molecular pharmacologic studies in the literature to date point to SSTR2, -3, and -5 as prominent therapeutic targets. Notably, octreotide is selective for these subtypes with nanomolar affinity at SSTR2 and with 10- and 100-fold selectivity over SSTR5 and -3, respectively (Table 3). Based on a systemic endocrine mechanism of action, SSTR2 and -5 would be the key targets as both of these subtypes have been shown to inhibit GH-IGF1.[18–21] Octreotide blocks GH hypersecretion in patients, animal models, and in

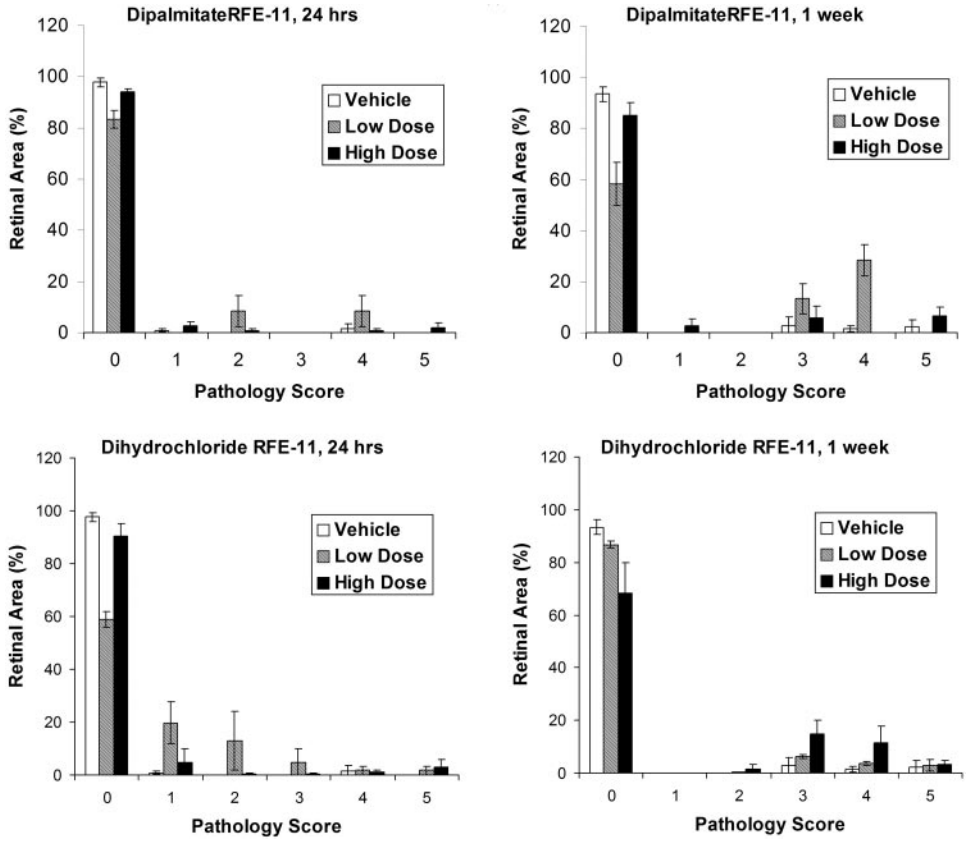

FIGURE 8. The distribution of pathology scores within each experimental group is shown after intravitreal administration of dipalmitate and dihydrochloride RFE-011. Two timepoints (24 hours and 1 week) and different concentrations of the drug formulations were tested and found to be well tolerated. The pathology observed from all treatments was mild and consisted of subtle morphologic changes or minimal disruption of the retinal layers. Retinal cells were healthy-appearing with no evidence of cell necrosis. In intravitreal toxicity studies, no significant disease was found with either formulation of RFE-011. Dipalmitate-RFE-011 results after 24 hours (*top left*) and 1 week (*top right*). Dihydrochloride-RFE-011 results after 24 hours (*bottom left*) and 1 week (*bottom right*). Pathology scores: 0, no pathology observed, the retinal layers are well organized; 1, minor breaks in the retinal layers, minor vacuolization with normal surrounding tissue, no necrosis observed; 2, clear disruption of integrity of the retinal layers and a higher level of vacuolization; 3, clear disruption of layer integrity with more pronounced changes than those for score 2, with a higher level of vacuolization and a degree of retinal dysplasia; 4, abnormal morphologic formations, loop-shaped or circular with normal surrounding tissue; 5, similar to score 4 but with more abnormal morphologic formations, circular in shape, and a higher degree of abnormality than retinas assigned score 4. Again, the surrounding tissue may look normal.

cell culture studies at nanomolar to sub-nanomolar concentrations, consistent with a tightly coupled functional response to the high affinity for SSTR2 and potentially also to SSTR5.

With regard to a direct antiangiogenic mechanism of action, SSTRs have been identified on endothelial cells and angiogenic vessels in several systems.[22,23] Woltering[24] reported that SSTR2 is selectively expressed in proliferating human placental vein endothelial cells relative to quiescent or resting cells. Also, SSTR2 expression was observed on peritumoral vessels of patients with cancer[25,26] and ocular vessels of patients with CNV.[22] Before this study, SSTRs have not been comprehensively and rigorously examined on HRECs, the cell type relevant to PDR. Based on the quantitative expression analysis described herein on SSTR1–5 in target HRECs, direct angiogenesis-inhibiting drug targets are confined to the SSTR1, -2, and -3 subtypes.

Direct antiangiogenic function has been demonstrated in vitro for octreotide, which has been shown to inhibit proliferation of HRECs, bovine choriocapillary endothelial cells, and human umbilical vein endothelial cells (HUVECs).[24,27] Similarly, octreotide has antiangiogenic activity in the chick chorioallantoic membrane and in the human placental vein physiological models.[23,28] As mentioned earlier, the functional effect has generally been attributed to SSTR2 receptor activation based on octreotide's activity as an SSTR2-selective agonist. However, octreotide's antiangiogenic effect requires micromolar to submicromolar concentrations, well above the nanomolar binding affinity at SSTR2 and the nanomolar concentrations that are functionally effective on GH release. Therefore, the SSTR3 receptor became of particular interest to us, since octreotide has micromolar affinity to SSTR3, consistent with the functional activity observed in angiogenesis models, and HRECs express SSTR3 receptors. Moreover, the clinical efficacy of octreotide in patients with ocular disease appears to require higher doses, and other groups have reported the involvement of SSTR3 in mediating antiangiogenic effects in other systems.[17]

To carefully delineate the contribution of SSTR2 vs. SSTR3, we used selective SSTR2 and -3 antagonists along with the NISA agonists. NISA compound RFE-007 inhibited HREC proliferation with an IC_{50} of 1 μM, similar to octreotide, whereas RFE-011 displayed a slightly greater IC_{50}. These results support SSTR2 as the functional mediator, since RFE-007 is highly selective for SSTR2 vs. SSTR3, with 1000-fold binding selectivity. Results in the HREC migration assay were also consistent with these findings. Furthermore, in the HREC tube formation assay RFE-007, octreotide, and somatostatin-14 inhibit with comparable potencies in the 100-nM concentration range. Of note, when HUVECs are used in a synthetic matrix (Matrigel; BD Biosciences) assay to test SSTR agonists, even lower concentrations of octreotide (10 nM) have been reported to be effective,[29] suggesting that tube formation is generally a more sensitive angiogenesis assay system, at least for somatostatin agonists.

The antiangiogenic effect using RFE-007 is better supported by an SSTR2 mechanism effect than by SSTR3 simply based on receptor affinity, which would require micromolar concentrations for SSTR3. Conversely, if an SSTR3 effect was predominant, we would have expected that somatostatin-14, which has nanomolar affinity to SSTR3, would have been more active than either RFE-007 or octreotide; however, it was equally active.

Our in vitro results thus indicate that SSTR2 receptors on HRECs mediate antiangiogenic functional effects by a signaling mechanism or cascade that is fundamentally less efficient than

GH inhibition via SSTR2 receptors on secretory cells. Thus, functional effects of NISAs targeting SSTR2 exhibit a two to three-magnitude right-shift in the dose–response curves with IC_{50}s that are greater than receptor binding of endocrine tissues. At this point, SSTR3 receptor antiangiogenic effects on HRECs may be less significant but cannot be ruled out completely. Previously, we had shown that a 100-nM SSTR3 selective agonist also inhibited HREC proliferation.[21] More selective and potent SSTR3 agonist tools are needed before this can be completely resolved.

The results from the in vivo efficacy studies are also consistent with a right-shifted SSTR2-mediated ocular antiangiogenic effect, as well as a direct ocular antiangiogenic mechanism of action. Although single-digit microgram/kilogram systemic doses and nanomolar plasma concentrations of octreotide and RFE-007 are effective at lowering GH, doses in the 1-mg/kg dose range were necessary for efficacy in the OIR mouse model. Although we have not titrated the efficacious drug concentrations in the OIR models, the 1-mg/kg dose given is consistent with plasma concentrations of octreotide and NISA in the micromolar range. For the lipophilic NISA compounds, we postulate ocular levels to be comparable to plasma levels. This in turn leads us to conclude, based on our OIR model, that octreotide is also relatively free to access the retinal ocular compartment and, therefore, that poor blood–retinal barrier penetration is not necessary to explain the high-dose requirement for octreotide in DR.

The results of the in vitro flux studies for RFE-011 clearly demonstrate that the compound diffuses across the sclera. The transscleral K_{trans} of solutes is known to be a function of molecular weight and molecular size.[14,30,31] The K_{trans} of 3.8×10^{-6} cm/s estimated for RFE-011 in the experiments of this study is well within the range that would be predicted by the compound's molecular weight.[31] By way of comparison, K_{trans} values for fluorescein (MW:332) and dexamethasone fluorescein (MW:841) determined with experimental procedures identical with those of the present study are 5.2×10^{-6} cm/s and 1.6×10^{-6} cm/s, respectively.[32]

The efficacy of RFE-011 in the CNV model after intravitreal administration provides conclusive support for the direct ocular mechanism of action and is also consistent with these results. Concentrations in at least the single-digit micromolar range and certainly orders of magnitude above nanomolar are projected from the efficacious intravitreal doses and are consistent with the in vitro and OIR results. The local intravitreal administration of the NISA compound RFE-011 was nontoxic, indicating that high-dose SSTR2 ocular drug therapy is intrinsically safe. Moreover, the in vitro human transscleral permeability of RFE-011 indicates that NISA compounds and SSTR2 agonist therapy may ultimately be amenable to less invasive transscleral administration.

Moreover, the use of NISA in combination with other agents may be the ideal therapeutic strategy. Combination therapy has proved to be a mainstream approach for treatment of cancer, AIDS, and other systemic diseases.[33,34] The multifactorial nature of PDR and CNV may lead to incomplete inhibition of neovascularization, making targeting a single cellular mechanism inadequate. Previously, we tested octreotide with casein kinase 2 inhibitors in the OIR model and found that the effect of the drug combination was significantly stronger than either single drug. Moreover, the use of the combination allowed us to achieve the same level of inhibition with markedly lower amounts of either agent.[35] Such additive result may be due to nonoverlapping networks of signaling pathways targeted by these two types of inhibitors.[36]

In summary, the antiangiogenic activity of NISA and octreotide is mediated by SSTR2 receptors via an overall much less efficient downstream coupling mechanism than is the neuroendocrine hormone (i.e., GH) release. As a result, direct ocular administration should be considered for future clinical studies using SSTR2 agonists for ocular neovascularization to ensure efficacious concentrations in the target tissue of the retina.

References

1. Frank RN. On the pathogenesis of diabetic retinopathy: a 1990 update. *Ophthalmology.* 1991;98:586–593.
2. Zimmer-Galler IE, Bressler NM, Bressler SB. Treatment of choroidal neovascularization: updated information from recent macular photocoagulation study group reports. *Int Ophthalmol Clin.* 1995;35:37–57.
3. Poulsen JE. Recovery from retinopathy in a case of diabetes with Simmonds' disease. *Diabetes.* 1953;2:7–12.
4. Reubi JC, Waser B, Liu Q, Laissue JA, Schonbrunn A. Subcellular distribution of somatostatin sst2A receptors in human tumors of the nervous and neuroendocrine systems: membranous versus intracellular location. *J Clin Endocrinol Metab.* 2000;85:3882–3891.
5. Grant MB, Guay C. Plasminogen activator production by human retinal endothelial cells of nondiabetic and diabetic origin. *Invest Ophthalmol Vis Sci.* 1991;32:53–64.
6. Grant MB, Khaw PT, Schultz GS, Adams JL, Shimizu RW. Effects of epidermal growth factor, fibroblast growth factor, and transforming growth factor-beta on corneal cell chemotaxis. *Invest Ophthalmol Vis Sci.* 1992;33:3292–3301.
7. Castellon R, Hamdi HK, Sacerio I, Aoki AM, Kenney MC, Ljubimov AV. Effects of angiogenic growth factor combinations on retinal endothelial cells. *Exp Eye Res.* 2002;74:523–535.
8. Florio T, Morini M, Villa V, et al. Somatostatin inhibits tumor angiogenesis and growth via somatostatin receptor-3-mediated regulation of endothelial nitric oxide synthase and mitogen-activated protein kinase activities. *Endocrinology.* 2003;144:1574–1584.
9. Poitout L, Roubert P, Contour-Galcera MO, et al. Identification of potent non-peptide somatostatin antagonists with sst(3) selectivity. *J Med Chem.* 2001;44:2990–3000.
10. Shaw LC, Afzal A, Lewin AS, Timmers AM, Spoerri PE, Grant MB. Decreased expression of the insulin-like growth factor 1 receptor by ribozyme cleavage. *Invest Ophthalmol Vis Sci.* 2003;44:4105–4113.
11. Smith LE, Wesolowski E, McLellan A, et al. Oxygen-induced retinopathy in the mouse. *Invest Ophthalmol Vis Sci.* 1994;35:101–111.
12. Sengupta N, Caballero S, Mames RN, Butler JM, Scott EW, Grant MB. The role of adult bone marrow-derived stem cells in choroidal neovascularization. *Invest Ophthalmol Vis Sci.* 2003;44:4908–4913.
13. Geroski DH, Edelhauser HF. Drug delivery for posterior segment eye disease. *Invest Ophthalmol Vis Sci.* 2000;41:961–964.
14. Olsen TW, Edelhauser HF, Lim JI, Geroski DH. Human scleral permeability: effects of age, cryotherapy, transscleral diode laser, and surgical thinning. *Invest Ophthalmol Vis Sci.* 1995;36:1893–1903.
15. Rudnick DE, Noonan JS, Geroski DH, Prausnitz MR, Edelhauser HF. The effect of intraocular pressure on human and rabbit scleral permeability. *Invest Ophthalmol Vis Sci.* 1999;40:3054–3058.
16. Boehm BO, Lang GK, Jehle PM, Feldman B, Lang GE. Octreotide reduces vitreous hemorrhage and loss of visual acuity risk in patients with high-risk proliferative diabetic retinopathy. *Horm Metab Res.* 2001;33:300–306.
17. Grant MB, Mames RN, Fitzgerald C, et al. The efficacy of octreotide in the therapy of severe nonproliferative and early proliferative diabetic retinopathy: a randomized controlled study. *Diabetes Care.* 2000;23:504–509.
18. Davis MI, Wilson SH, Grant MB. The therapeutic problem of proliferative diabetic retinopathy: targeting somatostatin receptors. *Horm Metab Res.* 2001;33:295–299.
19. Garcia de la Torre N, Wass JA, Turner HE. Antiangiogenic effects of somatostatin analogues. *Clin Endocrinol (Oxf).* 2002;57:425–441.
20. Sall JW, Klisovic DD, O'Dorisio MS, Katz SE. Somatostatin inhibits IGF-1 mediated induction of VEGF in human retinal pigment epithelial cells. *Exp Eye Res.* 2004;79:465–476.

21. Wilson SH, Davis MI, Caballero S, Grant MB. Modulation of retinal endothelial cell behaviour by insulin-like growth factor I and somatostatin analogues: implications for diabetic retinopathy. *Growth Horm IGF Res.* 2001;11(suppl A):S53–S59.
22. Lambooij AC, Kuijpers RW, van Lichtenauer-Kaligis EG, et al. Somatostatin receptor 2A expression in choroidal neovascularization secondary to age-related macular degeneration. *Invest Ophthalmol Vis Sci.* 2000;41:2329–2335.
23. Watson JC, Balster DA, Gebhardt BM, et al. Growing vascular endothelial cells express somatostatin subtype 2 receptors. *Br J Cancer.* 2001;85:266–272.
24. Woltering EA. Development of targeted somatostatin-based antiangiogenic therapy: a review and future perspectives. *Cancer Biother Radiopharm.* 2003;18:601–609.
25. Kumar U, Grigorakis SI, Watt HL, et al. Somatostatin receptors in primary human breast cancer: quantitative analysis of mRNA for subtypes 1–5 and correlation with receptor protein expression and tumor pathology. *Breast Cancer Res Treat.* 2005;92:175–186.
26. Reubi JC, Horisberger U, Laissue J. High density of somatostatin receptors in veins surrounding human cancer tissue: role in tumor-host interaction? *Int J Cancer.* 1994;56:681–688.
27. Grant MB, Caballero S, Millard WJ. Inhibition of IGF-I and b-FGF stimulated growth of human retinal endothelial cells by the somatostatin analogue, octreotide: a potential treatment for ocular neovascularization. *Regul Pept.* 1993;48:267–278.
28. Woltering EA, Barrie R, O'Dorisio TM, et al. Somatostatin analogues inhibit angiogenesis in the chick chorioallantoic membrane. *J Surg Res.* 1991;50:245–251.
29. Danesi R, Del Tacca M. The effects of the somatostatin analog octreotide on angiogenesis in vitro. *Metabolism.* 1996;45:49–50.
30. Ambati J, Canakis CS, Miller JW, et al. Diffusion of high molecular weight compounds through sclera. *Invest Ophthalmol Vis Sci.* 2000;41:1181–1185.
31. Prausnitz MR, Noonan JS. Permeability of cornea, sclera, and conjunctiva: a literature analysis for drug delivery to the eye. *J Pharm Sci.* 1998;87:1479–1488.
32. Kao JC, Geroski DH, Edelhauser HF. Transscleral permeability of fluorescent-labeled antibiotics. *J Ocul Pharmacol Ther.* 2005;21:1–10.
33. Haskell CM, ed. *Cancer Treatment*. 5th ed. Philadelphia: W.B. Saunders Co;2001:62–86.
34. Habtemariam T, Yu P, Oryang D, et al. Modelling viral and CD4 cellular population dynamics in HIV: approaches to evaluate intervention strategies. *Cell Mol Biol* (*Noisy-le-grand*). 2001;47:1201–1208.
35. Kramerov AA, Saghizadeh M, Pan H, et al. Expression of protein kinase CK2 in astroglial cells of normal and neovascularized retina. *Am J Pathol.* 2006;168:1722–1736.
36. Afzal A, Shaw LC, Ljubimov AV, Boulton ME, Segal MS, Grant MB. Retinal and choroidal microangiopathies: therapeutic opportunities. *Microvasc Res.* 2007;74:131–144.